Thermal Transpiration at the Microscale: A Crookes Cantilever

A. Passian,* R. J. Warmack, T. L. Ferrell, and T. Thundat
Oak Ridge National Laboratory, Oak Ridge, Tennessee 37831

(Received 11 November 2002; published 28 March 2003)

Local temperature inhomogeneities in systems containing micron and submicron objects can result in unexpected consequences. If the mean free path of the host gas constituents is comparable to a characteristic length of the system, then a net exchange of momentum occurs between the constituents and the involved surfaces. For a given temperature gradient and a given pressure range, this results in the presence of Knudsen and Knudsen-like forces (KF). The pressure dependence of these forces has been studied using a microelectromechanical system composed of a microcantilever near a substrate surface. Nano-Newton scale KF are observed by the bending of the microcantilever as monitored by the charge variation on the microcantilever-substrate assembly in a capacitive mode.

DOI: 10.1103/PhysRevLett.90.124503 PACS numbers: 47.45.Nd, 47.45.Dt, 47.45.Gx, 68.37.Ps

The macroscopic manifestation of thermal transpiration, first observed by Reynolds [1] in 1871, has had a remarkable history and continues to play an important role in many branches of modern science such as in the field of microelectromechanical systems (MEMS). This is evident from its long journey from the original work of Maxwell [2] in 1879, Knudsen [3,4] in 1909, and Einstein [5] in 1924 on the origin of the radiometric forces, to the recent somewhat fanciful ideas of a flying craft in the mesosphere [6–8], and of an engineless micromotor as proposed in this Letter.

Appearing parallel to Brownian disturbances, the anomalous fluctuations in microbalance weight measurements [9] and precise testing of the equivalence principle carried out in space missions [10] due to the seemingly omnipresent temperature inhomogeneities in the ambient residual gas and along the surfaces of the measuring devices are other implications of thermal transpiration.

The observation of the repulsion of small suspended bodies in a gas upon exposure to light was first made by Fresnel in 1825. Half a century later in 1873, this phenomenon was further studied by Crookes [11] using his radiometer [12,13]. Maxwell's explanation for the radiometric forces [2] was based on the phenomenon of thermal creep [14] of the gas molecules arising from the presence of temperature gradients along the solid surface. This motion of the gas, facilitating the thermal transpiration, occurs in a thin layer adjacent to the solid surface and results in the formation of a pressure gradient [15]. Momentum exchange of such flows with the edges of the vanes of a Crookes radiometer causes them to rotate with the heated side retreating from the light source. The aim of this Letter is to study the magnitude of various momentum exchange processes at microscale.

The degree of the competition between intermolecular collisions versus molecule-surface collisions at a characteristic length scale d can be characterized at temperature T and pressure P with the local value of the dimensionless Knudsen number $\mathrm{Kn} = \alpha\sqrt{T}/Pd$, where α is a molecule specific constant [4]. In particular, when studying MEMS with a characteristic length scale ranging from a fraction of a micrometer to several micrometers, the Kn is an important parameter in determining the onset and the magnitude of local pressure dependent processes such as Knudsen forces (KF) [16].

Here we present the first results of the investigation of the free motion of a boron doped U-shaped polysilicon microcantilever (Fig. 1), with dimensions similar to that used in atomic force microscopy (AFM), near a semiconductor surface during thermal transpiration. By capacitively monitoring the dynamics of the cantilever, it is shown that the presence of the nano-Newton KF results in a static deflection. This temperature and pressure dependent effect is measured in gases with various molecular composition in the Kn ranges (i.e., pressure ranges for the same d and T) from continuum ($\mathrm{Kn} \to 0$) through slip-flow ($0.1 > \mathrm{Kn} > 10^{-3}$) and transition ($10 > \mathrm{Kn} > 0.1$) to free-molecular ($\mathrm{Kn} > 10$) regimes. The observed behavior in the molecular regime agrees well with our theoretical predictions, while the overall subatmospheric pressure dependence is shown to be described by a semiempirical function. Though KF are extremely small in most cases, there exist situations where these forces can be large. These results are important for the optical devices at the subwavelength scale, for operation of microsensors, and in AFM whenever the Kn is such that thermal transpiration prevails.

It is well known [17] that the no-slip velocity boundary condition of the Navier-Stokes equations breaks down when the flow system is characterized with a $\mathrm{Kn} > 10^{-3}$ (below which the medium can be considered as continuum, i.e., ordinary density levels). When the Kn is in the near continuum and transitional regions, the first-order slip boundary condition accounts for the thermal-creep contribution via an additive term proportional to the temperature gradient of the surface. When the temperature gradient and its accompanying pressure gradient are not too large, Loyalka [18] calculated, by linearizing the Boltzmann equation, the longitudinal and transversal KF on the cylindrical surfaces of a hanging

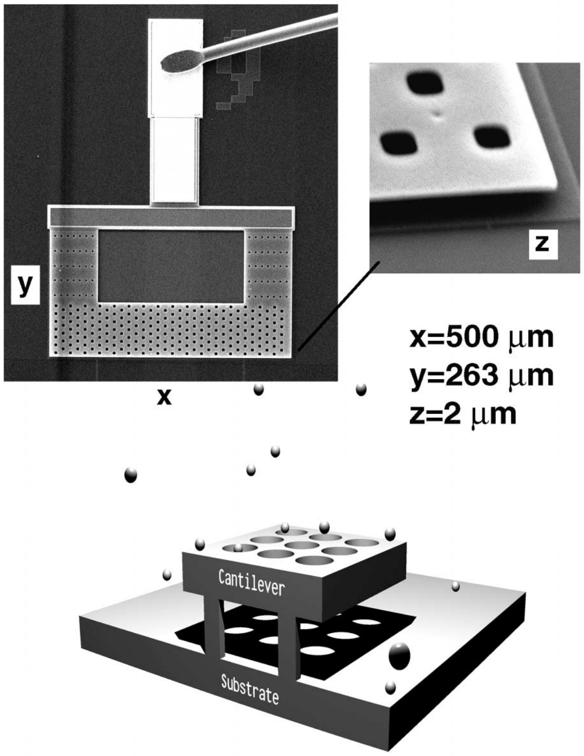

FIG. 1. Surface-micromachined cantilever. Polysilicon, doped and electrically conductive, is deposited on a silicon-nitride-coated silicon wafer to form the cantilever structure. Scanning electron micrograph (top) and schematic (bottom) of the capacitive cantilever assembly. The top left image shows the overall top view of the cantilever with its lower right corner magnified and shown in the top right image, where $z = d_0 = 2\ \mu$m is the nominal gap size. The schematic in the bottom depicts the microcantilever (including its embedded holes) "suspended" from the two anchors over the substrate.

wire of a vacuum microbalance. The calculated forces were shown [18] to exhibit maximum in the transition region in accordance with the reported data [9,19].

We calculate the KF for our case using a molecular model based on the solution of the Boltzmann equation in the free-molecular (low pressure) regime. In the absence of intermolecular encounters in this limit, the collision term vanishes from the Boltzmann equation [20] leaving it as $\mathcal{L}f(\mathbf{x}, \mathbf{c}, t) = 0$, where $\mathcal{L}$ is the differential operator of the Boltzmann equation neglecting external forces such as gravity, and f represents the distribution of the molecules with velocity $\mathbf{c}$ at location $\mathbf{x}$ at time t. From the solutions to this equation, Wu [21–23] showed that Knudsen's thermal transpiration invariance $P_i T_i^{-1/2}$ [4] must be modified to account for the departure of f from an isotropic distribution and can be written as $P_i I_i T_i^{-1/2}$, where $I_i = I(\mathbf{x}_i) = 4\pi(\iint_\Omega T_\Omega^{-1/2}\, d\Omega \times \iint_\Omega T_\Omega^{1/2}\, d\Omega)^{-1/2}$ measures the local deviation from the isotropicity, and T_Ω is the temperature of the molecules in the direction specified by the solid angle $d\Omega$ in the velocity phase space at $\mathbf{x}_i$ [20]. Measuring the extent to which kinetic energy is exchanged with the solid surface during a molecule-surface collision by assuming different energy accommodation coefficients [12] for the top a_{ct} and bottom a_{cb} surfaces of our microcantilever with a uniform temperature T_c, and the top surface a_s of the underlying substrate at T_s, we apply the above invariance to the regions (1) between the cantilever and the substrate, (2) immediately above the cantilever, and (3) far from the cantilever. The effect of each collision is then to thermalize the particle according to a diffuse reflection relation. Bypassing the details of the calculations [16], an integration over the pressure variation in the neighborhood of the cantilever then yields for the Knudsen pressure $\mathcal{K}$ the linear relation $\mathcal{K}(\tau_s, \tau_c, P) = g(\tau_s, \tau_c)P$, where P and T are, respectively, the pressure and temperature of the ambient medium, and the dimensionless function g is given by $g = (1/2)\sum_{i=0}^{3}\sqrt{u_i}$, with

$$u_0 = \frac{a_s\tau_s + a_{cb}(1 - a_s)\tau_c}{a_s + a_{cb} - a_s a_{cb}},$$
$$u_1 = \frac{a_{cb}\tau_c + a_s(1 - a_{cb})\tau_s}{a_s + a_{cb} - a_s a_{cb}},$$

$u_2 = 1 - a_{ct} + a_{ct}\tau_c$, and $u_3 = 1$. Here $\tau_s = T_s/T$ and $\tau_c = T_c/T$ denote the relative temperatures of the substrate and the cantilever, respectively. Note that the above are appropriate only for the free-molecular region. At higher pressures, equilibrium is established on both sides of the cantilever, which diminishes the effect. Consequently, a peak deflection occurs somewhere in the transitional regime.

Thus, for fixed (a_i, T_i) with i spanning the substrate, the cantilever, and the rest gas, the function $g = \partial\mathcal{K}/\partial P$ is a constant, and the force varies linearly with the pressure in the rarefied regime, that is, so long as, at our characteristic scale of $d \leq 2.0\ \mu$m, P is such that $\mathrm{Kn}(P) > \mathrm{Kn}(P_m)$ where P_m is a maximum pressure beyond which the effect of intermolecular collisions will be non-negligible in the surface-gas and gas-surface energy transport. The direction of the force on the cantilever is determined by g depending on the magnitude of the relative temperatures and the involved accommodation coefficients.

It can be shown [16,24] that, in the static limit, the bending W induced by the KF, at a point r along the cantilever, is given by $W(r) = \mathcal{K}R(r)/EI$, where $R(r) = r^4/24 - r^3/6 + r^2/4$, with the length of the cantilever normalized to unity, and E, I are the Young modulus and area moment of inertia, respectively. Thus, the capacitance yields a measure of W and the KF. The capacitance can then be calculated based upon the overlap differential area and local gap.

In our experiment, we used a custom-fabricated cantilever array chip. Two sets of holes of 8 and 2 μm diameter were made on the 2 μm thick cantilever as shown in Fig. 1 for an individual cantilever. The cantilever-substrate nominal separation distance is $d_0 = 2.0\ \mu$m. The chip was coupled to a custom-designed integrated circuit [25] which was then placed inside a vacuum bell jar system. A potential difference in form of a 0.6 V, 10 kHz waveform applied between the cantilever and the substrate allowed for the capacitance to be sensed at a rate of 10^4 s^{-1}. As a result, the gap size d could be sensed by the displacement current required to charge the cantilever capacitor. A mass flow controller and a mechanical pump were used to control the pressure of the residual gas which was determined with an absolute manometer. The 529 nm line of an argon ion laser was used to increase the temperature of the cantilever above the room temperature by (intensity modulated) focused illumination delivering a maximum power of 8 mW, measured at the plane of the cantilever.

The detected signals $S(P)$ from the lock-in amplifier are collectively presented in Fig. 2 for all the examined rest gases. The typical noise level in all the detected signals were less than 0.1 mV corresponding to a maximum deflection of $\delta d < 15$ Å. The effect of the Brownian fluctuations of the cantilever [26] is smaller than the noise level of the readout and is of no concern in our measurements. The radiation effects (infrared) are assumed to be small in our case. It can be shown [16] that in the blackbody limit the contribution of radiation to the heat transfer between the cantilever and the substrate is negligible.

Although the behavior of the results is clearly linear $S(P)|_{P\to 0} \propto P$ and inverse $S(P)|_{P\to\infty} \propto P^{-1}$ away from the observed peaks as seen in Figs. 2 and 3, the overall pressure dependence can be described with the following equation: $S_f(P) = a(bP^{\alpha} + cP^{-\beta})^{-1}$, where a, b, c, and $\alpha, \beta > 0$ are adjustable parameters. Noting that for α, β not too small $S_f|_{P\to 0} \to (a/c)P^{\beta}$, and $S_f|_{P\to\infty} \to (a/b)P^{-\alpha}$, the numerical fitting of the data to this equation for He, Ar, O_2, and CO_2 is shown in Fig. 3. The agreement is excellent just below atmosphere for the monatomic gases possessing only a translational degree of freedom as opposed to the polyatomics with the additional rotational and vibrational modes. In fact, if one is concerned only with the high Kn region, then $\beta = 1$ describes the data well for all the examined gases, and therefore $a/c \equiv g$ can be used to probe a variation in the accommodation coefficient of the cantilever surface material due to adsorption processes or use of various coatings. For example, g can be determined from the measurements for Ar and air to be 1.4×10^{-3} and 1.6×10^{-3}, respectively, which for the same relative temperature $\tau_c = 1.1$ will correspond to accommodation coefficients $a_i = a = 0.92$ and 0.90, respectively. The peak pressure in Fig. 3 can be determined by $P_{\max} = (c\beta/b\alpha)^{1/\alpha+\beta}$ to within the experimental precision for all the mono- and diatomic molecules examined, and with fair accuracy for CO_2. The equation for $S(P)$ approaches, in the limit $\alpha, \beta \to 1$, the semiempirical equation proposed by Brüche and Littwin [27,28]. Thus, the linear pressure dependence and the weak host gas dependence predictions of the equation for $\mathcal{K}$ (the only type dependence entering via the accommodation coefficients a_i) seem to be confirmed from the data presented in Fig. 2.

Figure 4 displays how the Knudsen signal in time domain varies with the modulation frequency of the laser, and how it can switch modes when the heating intervals are made shorter. The region labeled "I" in Fig. 4(b) prevails for longer exposure times where the entire

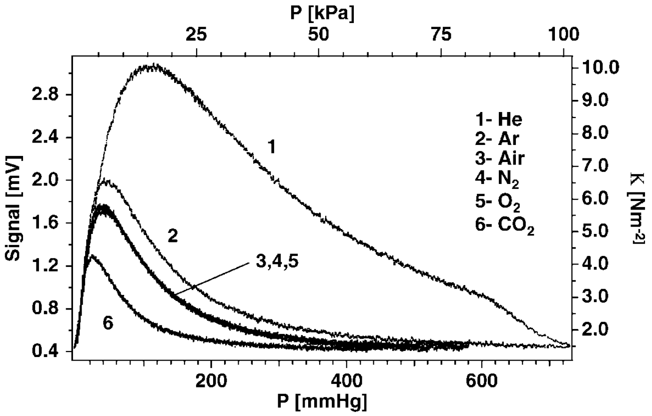

FIG. 2. The stress induced by the KF on the cantilever results in a static deflection which is sensed as a variation in the capacitance between the cantilever and the fixed substrate. The left axis displays the measured signal, while the right axis gives the corresponding Knudsen pressure yielding a total force in the range 90 nN ≤ KF ≤ 0.8 μN for the cantilever used. The examined residual gases furnishing the thermal transpiration yield different peaks due to their respective molecular compositions. The bending due to thermal stress in the cantilever appears as the gas independent baseline below 0.5 mV in the high and low Kn regions.

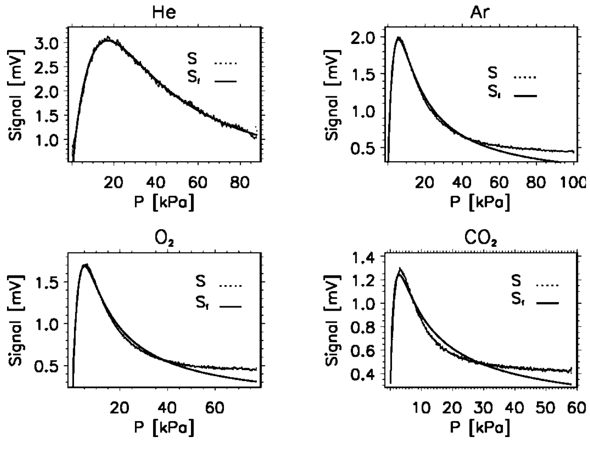

FIG. 3. The experimentally observed Knudsen effect (dotted curves) and the corresponding numerical fits (solid curves) to the function $S_f(P)$. The accuracy of locations of the peak pressure $P_{\max}$ obtained from $S_f(P)$ is excellent (within the experimental error) for the monatomic He and Ar, good for O_2, and fair for CO_2. The overall agreement is excellent in the respective regimes of free molecular motion for all the examined gases, but deteriorates in the lower Kn number regimes with increasing molecular degree of freedom.

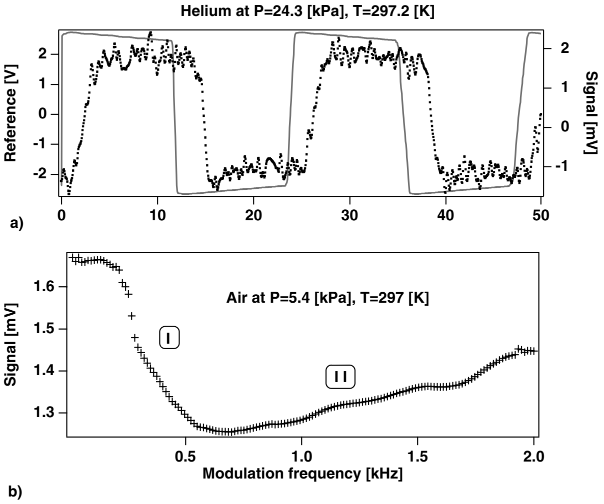

FIG. 4. The KF induced bending of the cantilever in time domain (a), and as a function of laser modulation frequency (b). (a) The 500 times averaged signal (dotted curve) representing the response of the cantilever, at a pressure close to the peak pressure for the Knudsen effect in helium, to the modulated laser beam represented by the reference signal of the lock-in (solid curve). (b) The variation of the signal with the laser modulation frequency in air at the peak pressure for the Knudsen effect. The shown behavior was observed for all the examined gases. The region labeled "I" corresponds to a decreasing temperature of the cantilever with increasing frequency (decreasing exposure time) up to high enough a frequency region labeled "II" for a cross sectional temperature gradient to be built up engaging the cavities (2 and 8 μm "pores," with the small pores being active in the smaller Kn region) embedded in the cantilever to participate in the thermal transpiration by exchanging momentum with the ambient molecules.

cantilever will reach a constant temperature, so that no contribution to the total KF is gained from the holes on the cantilever. As the chopping frequency is raised, T_c decreases along with the consequent KF. Further increase in the frequency (region II) creates a temperature gradient in the cantilever cross section, so that the holes in the cantilever contribute to the total KF, similar to Knudsen diffusion and thermal transpiration in media with isotropic microporosity. The higher the gradient, the higher the force. This is also consistent with the work of Liang [29] and its improved version of Takaishi *et al.* [30] for thermal transpiration in cylindrical geometry.

In summary, we have demonstrated that the KF can be measured with a microcantilever in the capacitive mode. The deflection of the cantilever due to this force was calculated in the free-molecular regime, and the results agree well with the observed effect. Presented measurements obey the semiempirical equation given by $S(P)$ for the entire pressure range. These results can be important when estimating the temperature and pressure ranges where the KF become important in microcantilever or other MEMS applications. Such measurements can also yield data on accommodation coefficients, difficult to obtain otherwise. The magnitude of the observed effect in the peak region suggests potential MEMS applications such as a cantilever based radiometer, a toothed wheel, and a temperature (pressure) gradient sensor.

The authors thank Marvin W. Dotson for technical support in the cantilever readout. This work was supported by the DOE-OBER and DOE-NN22. Oak Ridge National Laboratory, Oak Ridge, Tennessee, 37831-6123, is managed by UT-Battelle, LLC for the Department of Energy under Contract No. DE-AC05-0096OR22725.

---

*Email address: passianan@ornl.gov

[1] O. Reynolds, Philos. Trans. R. Soc. London **170**, 727 (1879).
[2] J. C. Maxwell, Philos. Trans. R. Soc. London **170**, 321 (1879).
[3] M. Knudsen, Ann. Phys. **31**, 144 (1967).
[4] M. Knudsen, *The Kinetic Theory of Gases* (Methuen & Co. LTD., London, 1950).
[5] A. Einstein, Z. Phys. **27**, 1 (1924).
[6] D. Jones, Nature (London) **392**, 337 (1998).
[7] D. Jones, Nature (London) **392**, 443 (1998).
[8] D. Jones, Nature (London) **395**, 120 (1998).
[9] J. M. Thomas and J. A. Poulis, *Vacuum Microbalance Techniques* (Plenum Press, New York, 1963).
[10] A. M. Nobili *et al.*, Phys. Rev. D **63**, 101101 (2001).
[11] P. Zeemann, Nature (London) **77**, 1 (1907).
[12] E. H. Kennard, *Kinetic Theory of Gases* (McGraw-Hill Book Company, Inc., New York, 1938).
[13] H. E. Marsh, E. Condon, and L. B. Loeb, J. Opt. Soc. Am. **11**, 257 (1925).
[14] G. Hettner, Z. Phys. **27**, 12 (1924).
[15] B. K. Annis, J. Chem. Phys. **57**, 2898 (1972).
[16] A. Passian *et al.*, J. Appl. Phys. **92**, 6326 (2002).
[17] M. Gad-El-Hak, *The MEMS Handbook* (CRC Press, New York, 2002).
[18] S. K. Loyalka, J. Chem. Phys. **66**, 4935 (1977).
[19] C. H. Massen *et al.*, *Vacuum Microbalance Techniques* (Plenum Press, New York, 1966).
[20] C. Cercignani, *Rarefied Gas Dynamics* (Cambridge University Press, Cambridge, 2000).
[21] Y. Wu, J. Chem. Phys. **48**, 889 (1968).
[22] Y. Wu, Ann. Phys. **7**, 21 (1966).
[23] Y. Wu, Ann. Phys. **7**, 144 (1967).
[24] W. C. Young, *Roark's Formulas for Stress and Strain* (McGraw-Hill Book Company, New York, 1989).
[25] C. L. Britton, Jr. *et al.*, Ultramicroscopy **82**, 17 (2000).
[26] I. Dorofeyev *et al.*, Phys. Rev. Lett. **83**, 2402 (1999).
[27] Von E. Brüche and W. Littwin, Z. Phys. **52**, 318 (1928).
[28] Von E. Brüche and W. Littwin, Z. Phys. **52**, 334 (1928).
[29] S. C. Liang, J. Appl. Phys. **22**, 148 (1951).
[30] T. Takaishi and Y. Sensui, Trans. Faraday Soc. **59**, 2503 (1963).